

ANGULAR MOMENTUM TRANSPORT IN THE SOLAR SUPERGRANULATION LAYER

Günther Rüdiger and Manfred Küker

Astrophysikalisches Institut Potsdam, 14482 Potsdam, Germany

ABSTRACT

The eddy viscosity in the solar supergranulation layer is derived from the observed rotational shear by computing theoretical rotation laws for the outermost parts of the solar convection zone using the results from numerical simulations of rotating convection as input. By varying the eddy viscosity, the results can be tuned to match the observations. The value of $1.5 \times 10^{13} \text{ cm}^2/\text{s}$ found for the eddy viscosity is considerably larger than the eddy magnetic diffusivity derived from the sunspot decay. The results are checked by comparison of the horizontal cross correlations of the velocity fluctuations with the observed Ward profile.

Key words: Hydrodynamics, Turbulence, Sun:rotation.

1. OBSERVATIONS

Sunspots rotate about 4% faster than the solar surface plasma at all latitudes. Helioseismology reveals a corresponding maximum of the angular velocity rather close to the surface, as shown in Fig. 1. Such a clear subrotation of the outermost layer of the convection zone is easiest understood as the result of angular momentum conservation of fluid elements with purely radial motions. In this domain of the solar convection zone, however, the gas motion is predominantly horizontal. Fluctuating fields with dominant horizontal intensity should simply produce superrotation rather than the observed subrotation (cf. Rüdiger 1989)

From the proper motions of sunspot groups, the faster of which tend to move toward the equator, Ward (1965) found the positive value of $\approx 0.1 \text{ (deg / day)}^2 \approx 2 \times 10^7 \text{ m}^2/\text{s}^2$ for the corresponding horizontal cross correlation on the northern hemisphere. More recent observations found smaller but always positive values (Nesme-Ribes, Ferreira, & Vince 1993).

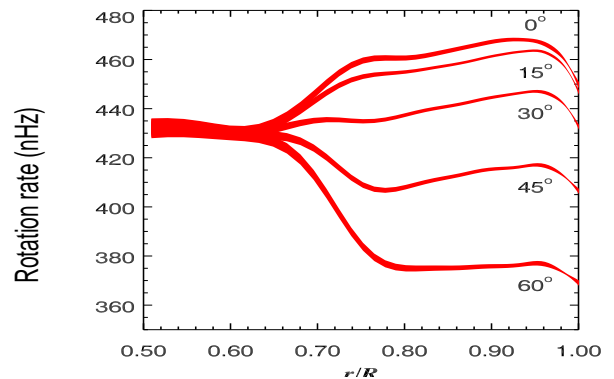


Figure 1. The internal solar rotation as found by helioseismology. Note the increase of the rotation rate with depth in the outermost layer. The maximum lies about 0.05 solar radii beneath the photosphere. (Graph courtesy NSF's National Solar Observatory).

2. THE REYNOLDS STRESS

The mean motion of a turbulent fluid is governed by the Reynolds equation,

$$\rho \left[\frac{\partial \bar{\mathbf{u}}}{\partial t} + (\bar{\mathbf{u}} \cdot \nabla) \bar{\mathbf{u}} \right] = -\nabla \cdot (\rho \mathbf{Q}) - \nabla p + \rho \mathbf{g}, \quad (1)$$

where

$$Q_{ij} = \langle u_i(\mathbf{x}, t) u_j(\mathbf{x}, t) \rangle \quad (2)$$

is the correlation tensor of the velocity fluctuations, \mathbf{u}' . Two components of the correlation tensor are relevant for the transport of angular momentum:

$$Q_{r\phi} = -\nu_T r \frac{\partial \Omega}{\partial r} \sin \theta + IV \sin \theta \quad (3)$$

$$Q_{\theta\phi} = -\nu_T \frac{\partial \Omega}{\partial \theta} \sin \theta + IH \cos \theta, \quad (4)$$

where ν_T is the eddy viscosity, Ω the rotation rate, V and H are dimensionless functions, and

$$I = \sqrt{\langle u_r'^2 \rangle \langle u_\phi'^2 \rangle}, \quad (5)$$

the turbulence intensity. The eddy viscosity and the turbulence intensity are related through

$$\nu_T = \frac{\tilde{\nu} I}{\Omega}. \quad (6)$$

In Eqs. 3 and 4, the terms containing ν_T describe the usual eddy viscosity part of the Reynolds stress while the non-diffusive terms containing I represent the Λ -effect, which drives the differential rotation.

To compute the rotation pattern, the quantities $\tilde{\nu}$, I , V , and H are needed. While the intensity I can be estimated from the convective velocity, as computed by mixing-length theory, $\tilde{\nu}$, V , and H have to be determined separately. Kitchatinov & Rüdiger (1993), and Kitchatinov, Pipin, & Rüdiger (1994) derived approximations using the second order approximation. Both the eddy viscosity and the Λ coefficients are functions of the Coriolis number,

$$\Omega^* = 4\pi \frac{\tau}{P_{\text{rot}}}, \quad (7)$$

where τ is the convective turnover time and P_{rot} the rotation period. For very slow rotation, $\Omega^* \ll 1$, angular momentum is transported outwards, and there is no horizontal Λ effect. For rapid rotation, the horizontal flux of angular momentum becomes dominant. The radial transport vanishes in the equatorial region and is negative at the poles.

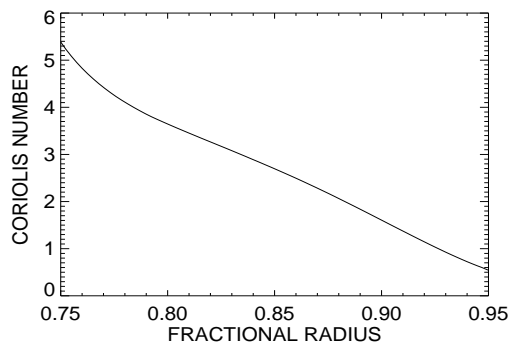


Figure 2. Coriolis number as function of the fractional radius in the bulk of the solar convection zone.

Figure 2 shows the variation of the Coriolis number with radius in the bulk of the solar convection zone, as computed with the model of Küker & Stix (2001). The Coriolis number is greater than unity in the bulk of the convection zone, but smaller in the granulation and supergranulation layers. Thus, by comparing the time scales of rotation and convection, we find that the bulk of the solar convection zone is rapidly rotating, while the uppermost layers are in a state of slow rotation.

The rotation laws derived with the expressions from Kitchatinov & Rüdiger (1993), and Kitchatinov, Pipin, & Rüdiger (1994) for the Reynolds stress reproduce the observations remarkably well in the bulk of the convection zone, but lack the negative radial shear in the supergranulation layer (Küker, Rüdiger, & Kitchatinov 1993, Kitchatinov & Rüdiger 1995, Küker & Stix 2001). We therefore follow a different approach to determine the parameters of the stress tensor in the uppermost part of the convection zone. Chan (2001) carried out 3D RHD simulations of rotating convection in f-planes. Figure 3 shows the V and H coefficients as function of the colatitude as derived from the simulations. The horizontal component

shows a strong peak at the equator, while the vertical angular momentum transport is strongest at the poles. Contrary to the predictions of Kitchatinov & Rüdiger (1993) for slowly rotating convection, the radial transport of angular momentum is directed inwards, and strongest close to the poles rather than at the equator. The horizontal transport exceeds the radial, and is strongly concentrated at low latitudes.

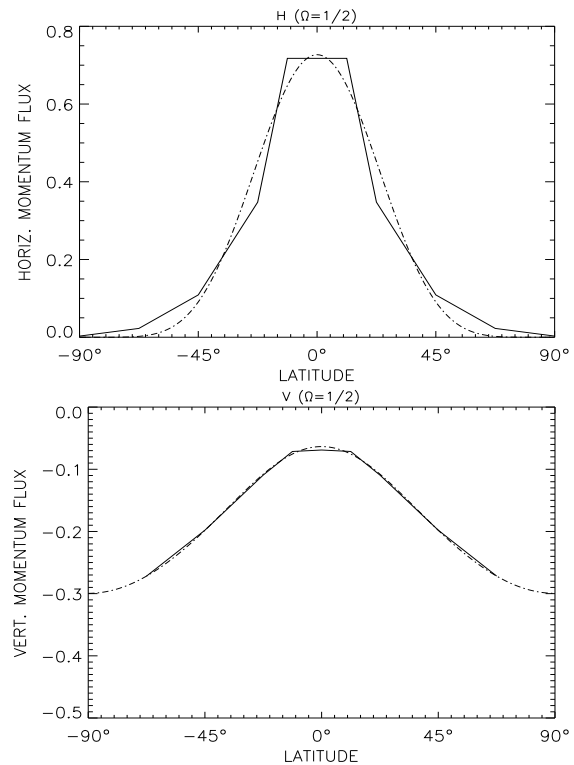


Figure 3. The horizontal (top) and vertical (bottom) components of the non-diffusive parts of the Reynolds stress, derived from RHD simulations. The dash-dotted lines denote the analytical fit used in the computations.

3. RESULTS

We solve the Reynolds equation using a time-explicit finite difference method for the outer 5% of the solar convection zone with the Reynolds stress as described above. As the horizontal shear is mainly generated in the bulk of the convection zone which has been excluded from the computations, we require

$$\Omega(\theta) = \Omega_0(0.7 + 0.3 \sin^2 \theta), \quad (8)$$

at the lower boundary. The upper boundary is assumed stress-free, i.e. $Q_{r\phi} = 0$.

In Eqs. 3 and 4, the intensity, I appears in the diffusive as well as in the non-diffusive part of the stress tensor. It therefore has no influence on the solution, which is stationary, but merely determines the time scale on which perturbations are damped. Fixing the average rotation period to 28 d, the only free parameter is the viscosity

parameter $\tilde{\nu}$, which is varied between 0 and 1 to get the best possible agreement between the computed and the observed rotation laws.

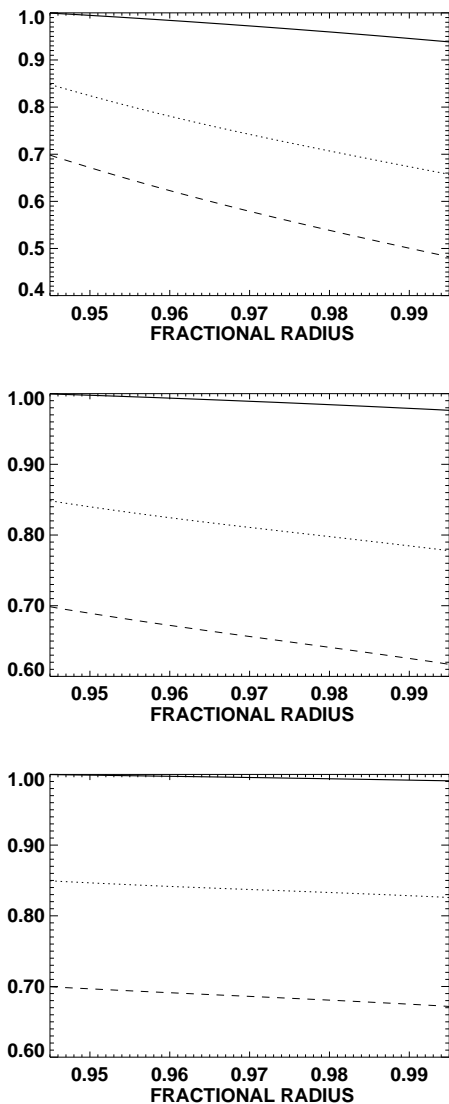


Figure 4. The normalized rotation rate at the equator (solid lines), 45 degrees latitude (dotted), and the poles (dashed) as a function of the fractional radius in the solar supergranulation layer as resulting from theory. From left to right: $\tilde{\nu} = 0.03, 0.1, 0.3$.

Figure 4 shows the rotation pattern for three different values of $\tilde{\nu}$. While, due to the lower boundary condition, there are no significant differences in the latitudinal shear, the radial shear strongly varies. Comparison with the observed profiles in Fig. 1 shows that the $\tilde{\nu} = 0.1$ case approximately matches the observations, while the $\tilde{\nu} = 0.03$ case produces too much, and the $\tilde{\nu} = 0.3$ case not enough shear. We conclude that $\tilde{\nu} = 0.1$ is the appropriate choice.

In Figure 5, the theoretical Ward profile,

$$W = -\frac{\tilde{\nu}}{\Omega} \frac{\partial \Omega}{\partial \theta} \sin \theta + H \cos \theta, \quad (9)$$

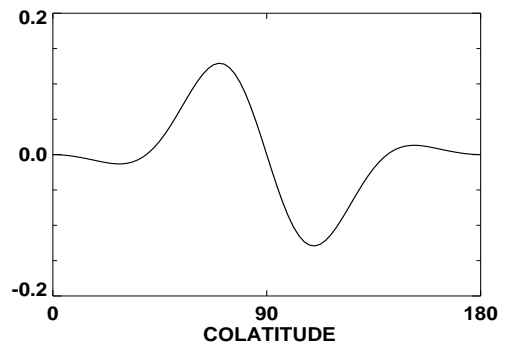


Figure 5. Theoretical Ward profile for $\tilde{\nu} = 0.1$.

of the surface rotation law is shown for $\tilde{\nu} = 0.1$. At low latitudes, the sign is positive in the northern and negative in the southern hemisphere. At higher latitudes, the sign is negative in the northern and positive in the southern hemisphere. In the equatorial region, the amplitude is roughly the same as that observed by Ward (1965), and the signs agree, too.

With a typical value of 200 m/s for the convection velocity in the supergranulation layer, a rotation rate $\Omega = 2.7 \times 10^{-6} \text{s}^{-1}$, and $\tilde{\nu} = 0.1$, we find

$$\nu_{\text{T}} \simeq 1.5 \times 10^{13} \text{cm}^2/\text{s} \quad (10)$$

for the eddy viscosity. This is two orders of magnitude larger than the value of $10^{11} \text{cm}^2/\text{s}$ derived for the magnetic diffusivity from sunspot decay. For the ratio between viscosity and magnetic diffusivity, the magnetic Prandtl number,

$$\text{Pm} = \frac{\nu_{\text{T}}}{\eta_{\text{T}}}, \quad (11)$$

we thus find a value as large as 150.

REFERENCES

- Chan K.L., 2002, ApJ 548, 1102
 Kitchatinov, L.L., Rüdiger, G., 1993, A&A 276, 96
 Kitchatinov, L.L., Pipin V.V., Rüdiger, G., 1994, Astron. Nachr. 315, 157
 Kitchatinov, L.L., Rüdiger, G., 1995, A&A 299, 446
 Küker M., Rüdiger, G., Kitchatinov, L.L., 1993, A&A 279, L1
 Küker, M., & Stix, M. 2001, A&A, 366, 668
 Nesme-Ribes E., Meunier N., Vince I., 1997, A&A 321, 323
 Rüdiger G., 1989, Differential rotation and stellar convection: sun and solar-type stars, Gordon and Breach Science Publishers
 Ward, F., 1965, ApJ 141, 543